

## Article

# Characterizing the Wake Effects on Wind Power Generator Operation by Data-Driven Techniques

Davide Astolfi <sup>1</sup>, Fabrizio De Caro <sup>2</sup>  and Alfredo Vaccaro <sup>2,\*</sup> 

<sup>1</sup> Department of Engineering, University of Perugia, Via G. Duranti 93, 06125 Perugia, Italy; davide.astolfi.green@gmail.com

<sup>2</sup> Department of Engineering, University of Sannio, Piazza Roma 21, 82100 Benevento, Italy; fdecaro@unisannio.it

\* Correspondence: vaccaro@unisannio.it

**Abstract:** Wakes between neighboring wind turbines are a significant source of energy loss in wind farm operations. Extensive research has been conducted to analyze and understand wind turbine wakes, ranging from aerodynamic descriptions to advanced control strategies. However, there is a relatively overlooked research area focused on characterizing real-world wind farm operations under wake conditions using Supervisory Control And Data Acquisition (SCADA) parameters. This study aims to address this gap by presenting a detailed discussion based on SCADA data analysis from a real-world test case. The analysis focuses on two selected wind turbines within an onshore wind farm operating under wake conditions. Operation curves and data-driven methods are utilized to describe the turbines' performance. Particularly, the analysis of the operation curves reveals that a wind turbine operating within a wake experiences reduced power production not only due to the velocity deficit but also due to increased turbulence intensity caused by the wake. This effect is particularly prominent during partial load operation when the rotational speed saturates. The turbulence intensity, manifested in the variability of rotational speed and blade pitch, emerges as the crucial factor determining the extent of wake-induced power loss. The findings indicate that turbulence intensity is strongly correlated with the proximity of the wind direction to the center of the wake sector. However, it is important to consider that these two factors may convey slightly different information, possibly influenced by terrain effects. Therefore, both turbulence intensity and wind direction should be taken into account to accurately describe the behavior of wind turbines operating within wakes.

**Keywords:** wind energy; wind turbines; wakes; data analysis; SCADA; condition monitoring.



**Citation:** Astolfi, D.; De Caro, F.; Vaccaro, A. Characterizing the Wake Effects on Wind Power Generator Operation by Data-Driven Techniques. *Energies* **2023**, *16*, 5818. <https://dx.doi.org/10.3390/en16155818>

Academic Editors: Marialaura Di Somma, Jianxiao Wang and Bing Yan

Received: 12 July 2023

Revised: 31 July 2023

Accepted: 2 August 2023

Published: 5 August 2023



**Copyright:** © 2023 by the authors. Licensee MDPI, Basel, Switzerland. This article is an open access article distributed under the terms and conditions of the Creative Commons Attribution (CC BY) license (<https://creativecommons.org/licenses/by/4.0/>).

## 1. Introduction

Wake interactions between nearby wind turbines represent the most important cause of producible energy loss in an operating wind farm. It is well known that the wind intensity downstream of a rotor gets reduced and that, if nearby wind turbines are not sufficiently spaced, the velocity deficit does not completely recover, thus affecting power production. In particular, on the one hand for offshore installations, it is convenient to maintain the layout of a wind farm as sufficiently compact to reduce Operation and Maintenance (OandM) costs but, on the other hand, if the layout is too compact the wake losses might reach 10–20% of the Annual Energy Production (AEP) [1,2].

In this regard, the offshore Lillgrund wind farm has become a paradigmatic test case which has been extensively studied in the literature [3,4]. It is composed of 48 Siemens SWT-2.3-93 wind turbines, with 2.3 MW of rated power. The layout is approximately square and the lowest distances between nearby wind turbines are 3.3 and 4.3 rotor diameters. In [5], it is estimated that the wake effects account for a 28% AEP loss. Another paradigmatic test case is the Horns Rev wind farm [6–9]. In that wind farm, the turbine spacing is higher (7,

9.3, and 10.4 rotor diameters) and the particular interest of the test case is in the fact that the wind farm is very large (80 Vestas V80 wind turbines).

The behavior of wind turbines under wake is also a factor to be accounted for by Transmission System Operators (TSOs) because the increasing wind energy penetration requires wind power plants to provide ancillary services [10–12]. For example, in [13], a control algorithm is formulated to distribute the power contribution of each turbine to minimize the wake effects and thus maximize the power reserve. On the other way round, if a wind turbine is requested to provide frequency support services, its wake behavior is affected [14]. Taking into account the wake effects is also an improvement for short-term wind power forecasts [15,16], which have crucial importance in electrical grid management.

Given this premise, it is evident that the analysis of wind turbine wakes is a topic that has attracted an extremely vast amount of literature, dealing with several aspects. Some of the most important are wind tunnel analysis [17–19], wind farm control [20,21], numerical simulations [22–26], and so on.

Nevertheless, some aspects are overlooked in the literature, namely those dealing with the exploitation of wind turbine Supervisory Control And Data Acquisition (SCADA) data [27,28] for the characterization of wind turbine operation under wake. To the best of the authors' knowledge, there are only a few papers on the topic. In [29], the authors relate meteorological data from a long-range lidar measurement campaign to the key SCADA parameters of offshore wind turbines. The main result of the work is that there is a good correlation between the standard deviation of the active power in the units of the average power, and in the ambient turbulence intensity (TI). Similar considerations are formulated in [30]. In [31], data-driven power curve models are formulated for a cluster of wind turbines extracted from a larger wind farm. It is shown that a graph model, accounting for wake interactions between wind turbines, largely diminishes the mismatch between model estimates and measurements.

Based on the aforementioned considerations, this paper aims to contribute to the identification of crucial SCADA parameters for characterizing wind turbine behavior in wake conditions. This work distinguishes itself from state-of-the-art ones in the type of employed data and in the methodologies. In particular, in [29,30], the fluctuations of wind turbine operation under wake are put in relation to meteorological data collected by a LiDAR. Yet, the use of this kind of sensor for wind farm OandM is at present still discouraged by economic considerations and it is therefore valuable to identify what can be understood by using solely SCADA data, as in this present work. The work in [31] moves from a consideration similar to the starting point of this work, which is the mismatch between nominal and real-world power curves in different environmental conditions [32]. In [33], a meaningful example is reported, which is the power curve of two wind turbines of the same model placed in different environments (moderately vs. highly turbulent). Those two curves appear remarkably different and this occurs not only for performance issues, but also because the measurement of the nacelle wind speed is a critical point. Not only are the nacelle wind speed measurements taken behind the rotor span and must be renormalized to estimate the free stream wind speed [34], but these measurements are also influenced by environmental conditions, including the turbulence generated by wake interactions. In fact, for example, the works of [35,36] highlight the effects of turbulence intensity on wind turbine power curves. Therefore, if on the one hand it is reasonable to construct power curve models taking into account the wake interactions (as done in [31]), on the other hand, for a deeper comprehension of the behavior of the wind turbines, it is meaningful to also consider curves based only on operation variables, developing further the approach used in previous studies such as [37].

Particularly, this work presents a real-world test case discussion using one year of SCADA data from an onshore wind farm located in Italy. The wind farm consists of nine turbines, each with a rated power of 3.3 MW. The turbine behavior under wake conditions is analyzed separately from operation under free stream conditions, based on the computation

of waked sectors defined by the International Electrotechnical Commission (IEC). Several meaningful test cases are then examined.

As an anticipation of the specific contributions collected in this study, it can be stated that, also using solely SCADA data, it is possible to highlight how turbulence intensity plays a significant role in determining notable differences in operational behavior under wake conditions. Recent state-of-the-art works confirm this view and analyze in detail the role of turbulence intensity by employing mainly numerical simulations [38,39]. It is therefore valuable to investigate what can be concluded in this regard through the analysis of a real-world industrial case. In this present work, turbulence intensity is shown to have a strong correlation with wind direction in the wake sector, meaning that the closer the wind direction aligns with the line connecting the involved turbines, the higher the turbulence intensity. However, this study demonstrates that these two variables, namely distance from the wake center and turbulence intensity, provide slightly different information. Therefore, a non-trivial insight achieved in this work is that both variables are required for accurate data-driven modeling of wind turbine power output in waked operations.

The structure of this paper is as follows: Section 2 provides a description of the employed methodology, whereas Section 3 analyzes the test case wind farm and the dataset. Section 4 discusses the obtained experimental results, and finally, Section 5 summarizes the main conclusions.

## 2. Methodology

### 2.1. The Data-Driven Approach

The methodology formulated in this work consists of several key steps, including the identification of the wake sector, characterization of wind turbine operation within the wake, and quantification of wake losses. Figure 1 provides an illustrative example of the target of the proposed methodology, showcasing a reference wind turbine generator (WTG) surrounded by two other WTGs. The red and green colored angular sectors represent the wake sectors of the reference WTG with respect to the neighboring WTGs (j-th and k-th). Particularly, these colored angular sectors are identified and analyzed to estimate the wake energy losses.

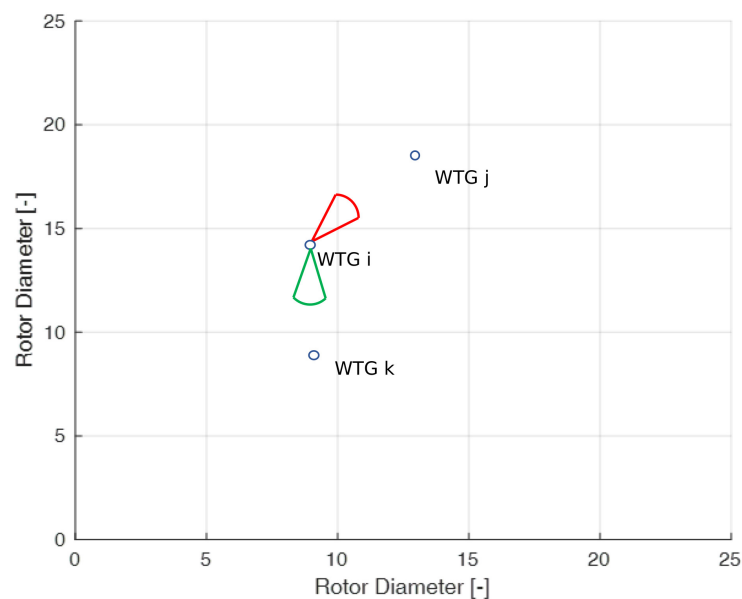


**Figure 1.** Visualization of wake sectors, where wind turbine i is affected by the operations of j (red) and k (blue).

The key steps of the proposed method go in sequence and proceed as follows:

- Identify the wake sectors by employing SCADA data (Section 2.2).

- Characterize the behavior of the wind turbines under wake through the analysis of appropriate operation curves (Section 2.3). This step is inspired by the IEC analysis of the power curve but generalizes it to further curves which are meaningful for the comprehension of the behavior under wake. Furthermore, this analysis allows for identifying limitations for the use of the power curve and therefore motivates the following step. Indeed, the nacelle wind speed measurements are affected by the amount of turbulence intensity and therefore it is unreliable to employ two average power curves measured under different conditions (e.g., in free stream vs. wake) to estimate the amount of power production loss caused by the wake.
- Formulate a reliable data-driven method for estimating the production loss caused by the wake interactions (Section 2.4.1). This is achieved by training a data-driven regression for the power of the target wind turbine as a function of the power of a reference wind turbine by using the free stream data. When simulating through the model the power of the target wind turbine when it is in wake, the quantification of the wake loss is substantially different from the model estimate (which is a simulation of the power that should have been produced if the wind turbine was not in wake) and the produced power.
- Employ the knowledge matured with the previous steps by formulating a method for characterizing, in general, the behavior under wake (Section 2.4.2). This step starts by employing only the measurements which are not biased by the presence of the wake. Namely, the nacelle wind speed measurements are excluded and only the operation variables and features elaborated from them are considered. A Sequential Features Selection is employed for identifying the key factors for describing accurately the power variability under wake.

## 2.2. Identification of the Wake Sectors

The center of a waked sector  $\theta_{ij}^{teo}$  is the direction connecting straightly two wind turbines  $i$  and  $j$  and the amplitude in degrees of the sector [40] is defined in Equation (1):

$$\alpha = 1.3 \frac{180 \arctan \left( 2.5 \frac{D}{L} + 0.15 \right)}{\pi} + 10, \quad (1)$$

where  $D$  is the rotor diameter and  $L$  is the distance between the wind turbines. For the sake of clarity, Figure 2 shows an example of  $\alpha$  and  $\theta_{ij}^{teo}$ . Through Equation (1), by elaborating the nacelle wind direction measurements, it is possible to establish if a wind turbine is operating in free stream or subjected to a single or multiple wakes. Namely, the procedure goes as follows:

- Consider a target  $i$ -th wind turbine;
- Set a counter to 0;
- For each wind turbine  $j = 1, \dots, N$ , where  $N$  is the number of wind turbines in the farm and  $j \neq i$ , compute  $\alpha_{ij}$  using Equation (1);
- For each wind turbine  $j = 1, \dots, N$ , where  $N$  is the number of wind turbines in the farm and  $j \neq i$ , compute the theoretical angle of the wake sector center as  $\theta_{ij}^{teo} = \arctan \frac{y_i - y_j}{x_i - x_j}$ ;
- If the nacelle wind direction  $\theta_i$  of the target  $i$ -th wind turbine is comprised in the interval  $[\theta_{ij}^{teo} - \frac{1}{2}\alpha_{ij}, \theta_{ij}^{teo} + \frac{1}{2}\alpha_{ij}]$ , increase the counter.

If, upon cycling  $j$  from 1 to  $N$ , the counter is 0, the measurement corresponds to the operation in the free stream of the  $i$ -th wind turbine. If the counter is 1, the operation is under a single wake (i.e., only of one wind turbine), and so on. In this study, only sectors of free stream operation and single wake have been considered, and the corresponding datasets are indicated in general as  $D_{free}$  and  $D_{wake}$ .

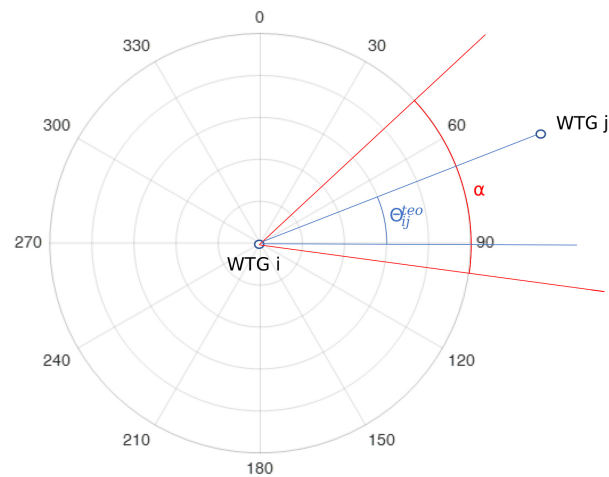


**Figure 2.** Visualization of  $\alpha$  and  $\theta_{ij}^{teo}$ .

### 2.3. Characterization of Wind Turbine Operation under Wake

The common ground for a general comprehension of the wind turbine behavior under wake is the generalization of the binning method, which the IEC has codified for the analysis of the power curve [41].

In the case of the power curve, the point is simply averaging the power measurements per interval of the nacelle wind speed. The amplitude of the bin is typically selected as 0.5 or 1 m/s. The former is selected in this work. Therefore, given  $N_j$  measurements occurring in the  $j$ -th bin of wind intensity, the average  $P_j$  is simply given in Equation (2):

$$P_j = \frac{1}{N_j} \sum_{i=1}^{N_j} P_{i,j} \quad (2)$$

where  $P_{i,j}$  is the  $i$ -th measurement occurring in the  $j$ -th bin. The average power curve is therefore given by the points  $(v_j, P_j)$ , where  $v_j$  is the center of the  $j$ -th wind speed bin. The data are pre-filtered from cut-in ( $v_{cut-in}$ ) to rated wind speed ( $v_{rated}$ ). In principle, other pre-processing methods could be necessary in case of power curtailments [42], but this is not the case for the selected wind farm.

The above method can be generalized by considering whatever couple of quantities  $(X, Y)$  whose relation is considered relevant. The principle is the same, i.e., averaging  $Y$  per interval of  $X$ .

In order to characterize the waked sectors, some features can be computed from the raw SCADA measurements, as, for example, the turbulence intensity, which is defined in Equation (3):

$$I = \frac{v_\sigma}{v} \quad (3)$$

as the ratio between the standard deviation ( $v_\sigma$ ) of the nacelle wind speed on a 10-minute time basis and the average wind speed ( $v$ ) on the same time interval.

Another meaningful feature that can be computed from the raw data is the angular distance between the center of the wake sector and the measured wind direction  $\theta$ . This quantity is defined in Equation (4):

$$\theta_d = \theta^{teo} - \theta. \quad (4)$$

The curves considered of interest for the purposes of this present work are therefore summarized in Table 1, where the range of  $X$  and the bin amplitudes are reported.

**Table 1.** Analyzed operation curves.

Curve	X	Y	X Range	X bin
Power Curve	$v$	$P$	$[v_{cut-in}, v_{rated}]$ m/s	0.5 m/s
Turbulence Intensity Curve	$v$	$I$	$[v_{cut-in}, v_{rated}]$ m/s	0.5 m/s
Rotor-Power Curve	$\omega$	$P$	$[\omega_{min}, \omega_{max}]$ rpm	0.5 rpm
Power-Blade Pitch Curve	$P$	$\beta$	$[0, P_{rated}]$ kW	$0.1 P_{rated}$
Angular Distance-Turbulence Intensity	$\theta_d$	$I$	$[\theta_c - 0.5\theta_a, \theta_c + 0.5\theta_a]$	$5^\circ$
Angular Distance-Residuals	$\theta_d$	$R$	$[\theta_c - 0.5\theta_a, \theta_c + 0.5\theta_a]$	$5^\circ$

The curves indicated in Table 1 have an intuitive explanation, except for those involving the use of the angular distance with respect to the center of the wake. The necessary details about the use of such a curve are reported in Section 4.

## 2.4. Characterization of the Waked Sectors and of the Wake Losses

### 2.4.1. Estimation of the Wake Losses

The computation of the wake losses needs an estimate of how much a wind turbine would have produced if it were not in wake. In this regard, the idea proposed in this work is learning this from the data by exploiting the fact that the wind turbines are grouped in clusters. Namely, the procedure goes as follows:

- Filter the data for the selected wind turbine pair where both turbines are operating in free stream conditions. To achieve this, as discussed in Section 2.2, ensure that for each turbine pair  $i$  and  $j$ , the wind directions  $\theta_i$  and  $\theta_j$  do not fall within any wake sector created by other turbines in the farm.
- Create a filtered dataset, denoted as  $D_{free}$ , containing the selected turbine pairs.
- Train a data-driven model with the power of the reference upstream wind turbine  $P_{upstream}$  as the input and the power of the target downstream wind turbine  $P_{downstream}$  as the output.
- Consider the dataset describing the downstream wind turbine affected by a single wake of an upstream one, referred to as  $D_{wake}$  for brevity.
- Use the trained model to simulate the output, denoted as  $y_{free}$ , by inputting the power of the reference wind turbine from the  $D_{wake}$  dataset.
- Compare the model estimates  $y_{free}$  with the actual measurements  $y$ .

The selected type of model is a Support Vector Regression (SVR) with Gaussian Kernel. It has been selected because it has desirable characteristics for this kind of application [43–45]: robustness to outliers, relatively fast convergence, and nonlinearity.

The rationale of this approach to the estimate of the wake losses is that, by training the model with the  $D_{free}$  dataset, the model learns the relation between the power of the reference and target wind turbines when both are in free stream. By feeding as input to the model the data  $D_{wake}$ , the model simulates how much the target wind turbine would produce if it were not in wake for a given power of the reference wind turbine (which is in a free stream in the  $D_{wake}$  dataset). In other words, the estimate of the wake losses can be retrieved from the difference between measurements and model estimates. In particular, the loss relative to the Annual Energy Production is estimated in Equation (5):

$$E_{perc.loss.} = \frac{\sum_{D_{wake}} y - y_{free}}{\sum_{D_{tot}} y}, \quad (5)$$

where  $y$  is the power measurements of the target wind turbine and  $y_{free}$  are the estimates of the model, which simulates the free stream data-driven relation. The numerator is the sum of the residuals in the  $D_{wake}$  dataset, while the sum at the denominator should be intended on the whole yearly dataset considered in this study (indicated as  $D_{tot}$ ).

#### 2.4.2. Features Classification

This analysis is aimed at identifying the key SCADA parameters which are required for a thorough characterization of the operation under wake. In general, in the wind power sector, there are several problems that can be stated as the necessity of determining the most relevant features for predicting an output which in general has a multivariate dependence on several factors [46]. In particular, for the present application, due to the critical points related to the wind speed measurements which are affected by the level of turbulence intensity, we have decided to employ only operation variables which are not affected by such kinds of biases. Namely, the starting set of features is listed in Table 2 and constitute a matrix of  $P$  features:  $\mathcal{X} = \{x_1, \dots, x_j, \dots, x_P\}$ . The amount of turbulence intensity is resembled in the variability of the operation variables, such as the rotational speed and blade pitch. Notice that this selection is quite standard, in that all the modern wind turbines collect the measurements needed to construct the features in Table 2. Therefore, the selection can be considered general and not linked to the specific test case.

**Table 2.** Starting set of features for the characterization of the operation under wake.

Rotor Speed (Average, Minimum, Maximum, Std Dev) $\omega$ (rpm)
Blade Pitch (Average, Minimum, Maximum, Std Dev) $\beta$ ( $^\circ$ )
Direction Distance with respect to the wake center $\theta_d$ ( $^\circ$ )

In order to classify the above features, these preliminary steps are applied:

- Select a portion of a waked dataset; reasonably, the most populated;
- Divide it in a training and testing portion (two-thirds and one-third);
- Feed the input variables of Table 2 in the training dataset to a sequence of SVRs whose output is the power of the downstream wind turbine in waked operation.

Thereafter, the importance of the features is classified through a Sequential Features Selection (SFS) algorithm, whose objective is determining sequentially what features provide a decrease in a loss function and by how much. At each round of the algorithm, the most desirable input variable to the model (and thus the most important feature at that round) is the one which, if added to the model, leads to the highest decrease in a loss function. The loss function selected in this work is the Root Mean Square Error (RMSE), which is defined in Equation (6):

$$\text{RMSE} = \sqrt{\frac{\sum_i^N (R[i] - \bar{R})^2}{N}}, \quad (6)$$

where  $R[i]$  is the  $i$ -th difference between measurement  $y$  and model estimates  $\hat{y}$  and  $\bar{R}$  are the average residual on the considered testing set. Namely, the precise steps of the SFS are the following:

- Initialize a matrix  $X_{M=0}$  with null dimensions to store the most significant predictors from the set  $\mathcal{X}_{M=0} = x_1, \dots, x_j, \dots, x_P$ , where  $P$  represents the number of input variables. Set a vector of output  $y$ , a counter variable  $M$  set to 1, and  $\text{RMSE}_{M=0}$  to  $\infty$ .
- Repeat until  $\text{RMSE}_M > \text{RMSE}_{M-1}$ :
  1. Iterate for each  $j$ -th variable  $x_j$ , where  $j \in [1, |\mathcal{X}_{M-1}|]$ :
    - (a) Divide the training set  $\mathcal{X}_{M-1}$  using  $K$ -fold cross-validation.
    - (b) For each  $k \in [1, \mathcal{K}]$ , build a SVR-based model using the  $k$ -th training set, and merge the variables of  $X_{M-1}$  with the  $j$ -th variable  $x_j$  in the set  $\mathcal{X}_{M-1}$ . Test each  $j$ -th model on each one of the  $\mathcal{K} - 1$  folds.
    - (c) Compute the average loss function across the  $\mathcal{K}$  sample-sets for each  $j$ -th model.
    - (d) Sort the  $|\mathcal{X}_{M-1}|$  models and select the variable from  $\mathcal{X}_{M-1}$  associated with the lowest loss function.

2. Remove the selected variable from  $\mathcal{X}_{M-1}$  and merge it with the variables in  $\mathcal{X}_{M-1}$  to create  $\mathcal{X}_M$ .
  3. Increase the counter  $M$  of one unit.
- End the algorithm when the loss function stops decreasing.

The interest in the application of this algorithm is twofold:

- The most meaningful features for modeling the power of the test case wind turbine in wake are identified using a particular dataset;
- One could employ the above features on other waked sectors and inquire how much the selected set is appropriate.

The selected accuracy metrics are the RMSE (defined in Equation (6)) and the Mean Absolute Error (MAE), which is defined in Equation (7):

$$\text{MAE} = \frac{1}{N} \sum_i^N |\mathbf{R}[i]|, \quad (7)$$

as simply the average of the absolute differences between model estimates and measurements.

### 3. Case Study

The test case wind farm features nine wind turbines with  $D = 117$  meters of rotor diameter. The machines have variable rotational speeds which are controlled through hydraulic blade pitch actuation. The rated power of each wind turbine is 3.3 MW. The wind farm is sited onshore on a gentle terrain and the layout is reported in Figure 3, where the inter-turbine distance is indicated in units of rotor diameters.

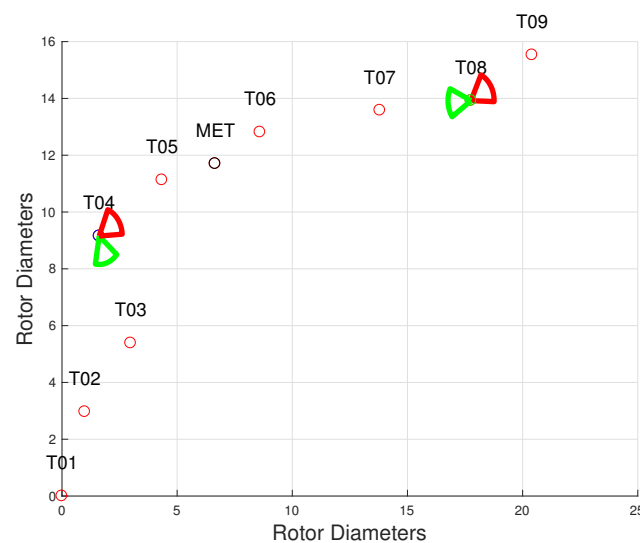


**Figure 3.** The layout of the selected wind farm. The target wind turbines are indicated, with the waked sectors with respect to the nearby ones.

The available SCADA-collected data have ten minutes of averaging time and go from 1 January to 31 December 2020. The measurement channels at disposal are listed in Table 3.

**Table 3.** SCADA-collected measurements at disposal for the study.

Nacelle wind speed $v$ (Average, Minimum, Maximum, Std Dev) (m/s)
Nacelle wind direction $\theta$ (Average) $^{\circ}$
Rotor Speed $\omega$ (Average, Minimum, Maximum, Std Dev) (rpm)
Blade Pitch $\beta$ (Average, Minimum, Maximum, Std Dev) $^{\circ}$
Active Power $P$ (Average, Minimum, Maximum, Std Dev) (kW)

### 3.1. Selection of the Wake Sectors

The waked sectors have been computed for each wind turbine with each other turbine in the farm. Based on these methods, the sectors indicated in Table 4 have been selected (and plotted in Figure 3) for the analyses of this work. In those sectors, the downstream wind turbine is under the wake of only one wind turbine, namely the upstream one indicated in Table 4.

Evidently, a wind turbine layout is designed in order to minimize the occurrence of operation under wake and therefore the waked sectors in general occur rarely. These target wind turbines (T04 and T08) have been selected because they were more characterized by the occurrence of measurements describing their operation under a single wake of a nearby wind turbine. The wind roses measured by the nacelle anemometer of T04 and T08 are indeed reported, respectively, in Figures 4 and 5, and the population of the sectors is reported in Table 4.

**Table 4.** Selected single wake sectors.

Sector Name	Upstream	Downstream	Center $\theta_c$	Amplitude $\theta_a$	N. Measurements
T04 North	T05	T04	54°	64.3°	1897
T04 South	T03	T04	160°	59°	5529
T08 North	T09	T08	58.7°	66.9°	1626
T08 West	T07	T08	265°	59.3°	1064

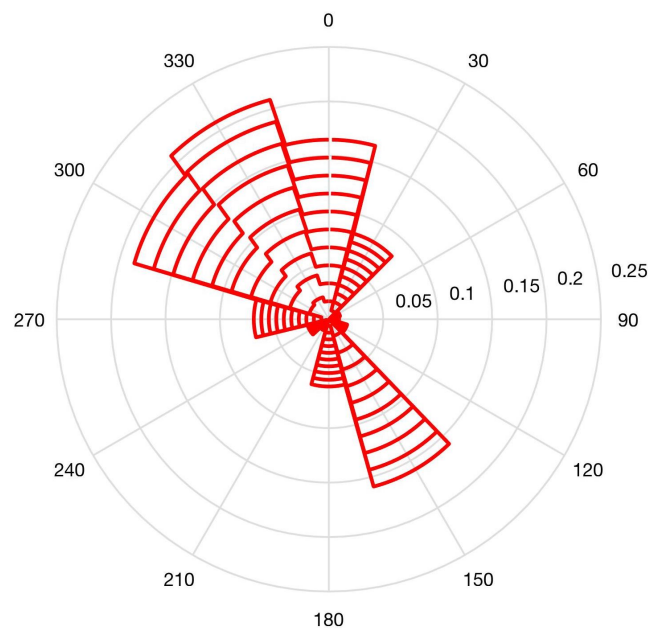


**Figure 4.** The wind rose measured by the T04 nacelle anemometer.

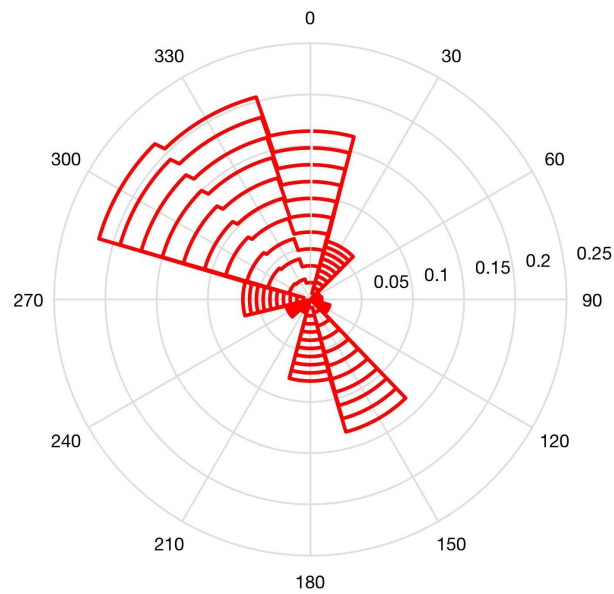


**Figure 5.** The wind rose measured by the T08 nacelle anemometer.

### 3.2. Operation Curves

In Table 5, the values of the  $X$  variables listed in Table 1 are reported for the specific case study of this work.

**Table 5.** Range of the variables for the operation curve analysis

Variable	Value
$v_{cut-in}$	4 m/s
$v_{rated}$	13 m/s
$\omega_{min}$	6 rpm
$\omega_{max}$	13 rpm
$P_{rated}$	2 MW

### 3.3. Estimation of the Wake Losses

In Table 6, the input and output variables of the model for the wake losses estimation are reported for the case of interest, in relation to Table 4 and Figure 3.

**Table 6.** Input and output for the data-driven model for estimating the wake losses.

Sector Name	Input	Output
T04 North	$P$ T05	$P$ T04
T04 South	$P$ T03	$P$ T04
T08 North	$P$ T09	$P$ T08
T08 West	$P$ T07	$P$ T08

### 3.4. Features Classification

For the selected case study, the features classification for the characterization of the operation under wake has been run using the T04 South case because it is the most populated (see Table 4). The crosscheck of the method has been pursued by computing accuracy metrics on two datasets: the testing part of the T04 South dataset and the T04 North dataset. This comparison is particularly interesting in this test case, in light of the different characteristics of these two waked sectors (which are discussed in detail in the following Section 4).

## 4. Experimental Results

### 4.1. Characterization of Wind Turbine Operation under Wake

Given the line of reasoning in [29], which is summarized in Section 1, the first analysis is inquiring if the selected waked sectors can be distinguished as regards the turbulence intensity. Therefore, in Figure 6, the average curve of the turbulence intensity as a function of the wind speed is reported for the four datasets of Table 4. Interestingly, it arises that for each target wind turbine, there is a sector with higher turbulence (T04 South and T08 North) and a sector with lower turbulence (T04 North and T08 West).

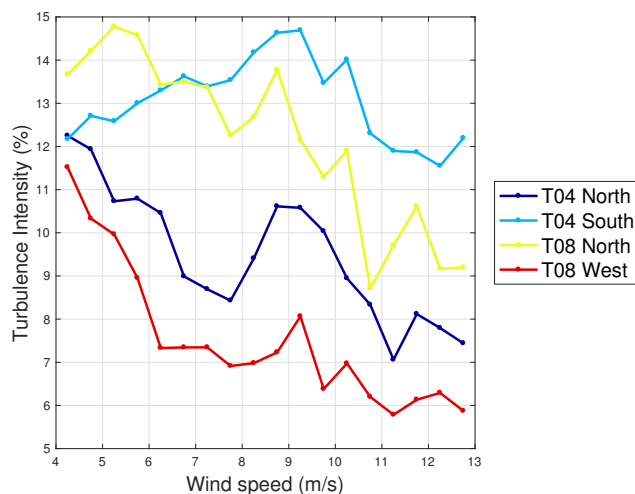


**Figure 6.** The average turbulence intensity for the two waked sectors for the two target wind turbines.

Therefore, in Figure 7 we investigate if there are differences related to the waked sectors in the most important operation curve, which of course is the power curve. For brevity, the curve for only T04 is reported, but the situation is similar also for T08. The interpretation of the power curve of Figure 7 is somehow counter-intuitive. From that curve, one would be led to argue that the power curve measured in wake is slightly better than in free stream and the effect is slightly higher for the waked sector with higher turbulence. Likely, as discussed for example in [33], the increased turbulent kinetic energy is not captured by the nacelle anemometer and this leads to an effect of under-estimation of the wind intensity. Therefore, the fact that the power curve in the waked sectors in Figure 7 looks slightly higher than in free stream is most likely due to wind speed measurement issues. This supports the fact that a consistent interpretation of wind turbine performance in complex conditions requires the analysis of further operation curves [37].

In Figures 8 and 9, two fundamental curves describing wind turbine operation are reported, which are the rotor speed-power and the power-blade pitch curve (see Table 1). From Figure 8, it arises that when there is higher turbulence (thus in wake), the extracted power for a given rotational speed is slightly higher. It looks as if, in the full aerodynamic load regime, higher turbulence for a given wind speed could even be slightly favorable for power extraction. From Figure 9, it arises that the average blade pitch does not change remarkably in wake or in free stream up to more or less 2 MW, which for this wind turbine model is the point at which the rotational speed saturates. When in partial aerodynamic load, if the turbulence is higher then the average blade pitch is also higher, which means that the aerodynamic efficiency is lower, and thus a higher incoming wind kinetic energy is required to extract a certain power output. In other words, the increased turbulence in waked operation is remarkably unfavorable in the partial aerodynamic load. An explanation of this behavior is that, when the wind turbine regulates the rotational speed and the blade pitch (full aerodynamic load), it can follow the rapid fluctuations induced by the wake in the form of increased turbulence. When the rotational speed is held fixed and only the blade pitch can vary (partial aerodynamic load), the wind turbine is not capable

anymore to follow the variability of the highly turbulent wind, and the efficiency of the power conversion is therefore lower.

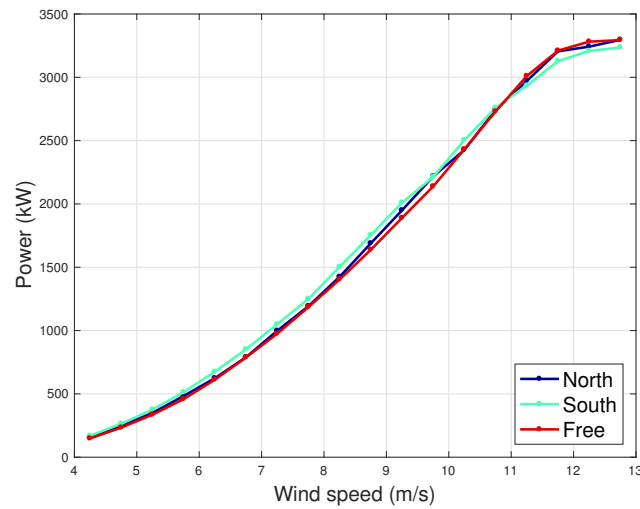


**Figure 7.** The average power curve for the target T04 wind turbine, for the two waked sectors, and for the free stream case.

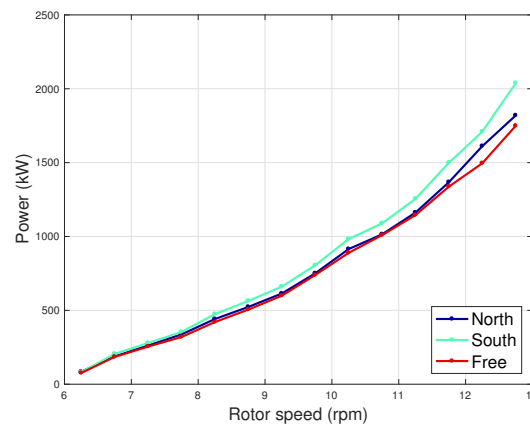


**Figure 8.** The average rotor speed-power curve for the target T04 wind turbine, for the two waked sectors and for the free stream case.

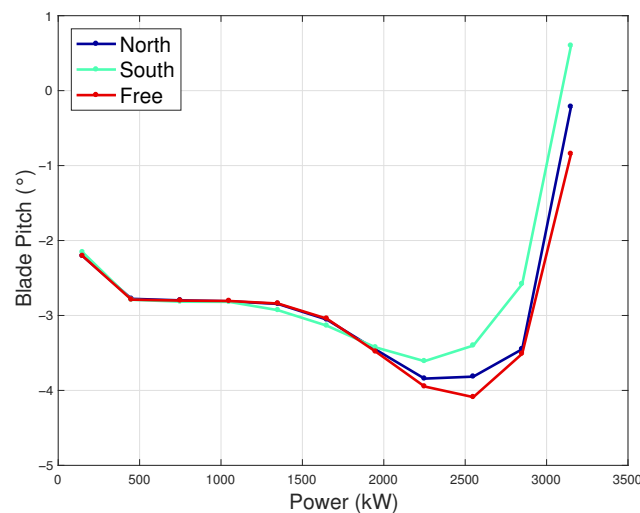


**Figure 9.** The average power-blade pitch curve for the target T04 wind turbine, for the two waked sectors, and for the free stream case.

#### 4.2. Characterization of the Waked Sectors and of the Wake Losses

A meaningful quantity for characterizing the operation under wake is how much the wind direction deviates with respect to the center of the wake (Equation (4)), i.e., to the values reported in Table 4. In Figure 10, we report the distribution of such a quantity for the four considered cases. The four waked sectors have quite different features. The T04 North case is completely skewed negatively, while T04 South is similar but with a non-negligible occurrence of measurements along the center of the wake. The T08 North has a practically uniform distribution from  $-30^\circ$  to  $+20^\circ$ , while the T08 West is completely positively skewed.

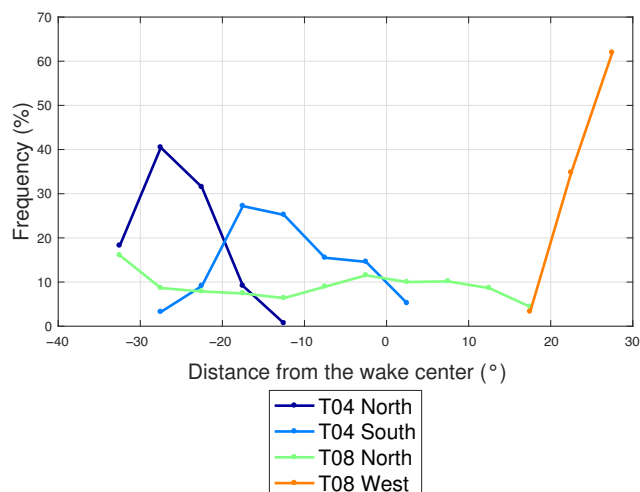


**Figure 10.** The distribution of distances from the center of the waked sectors for the four test cases.

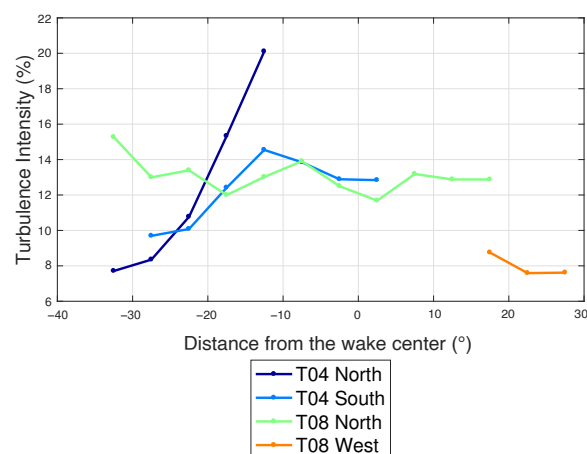
Figure 11 reports the average turbulence intensity as a function of the distance from the wake center for the four considered waked sectors. The turbulence intensity is measured through the nacelle anemometer of the turbine downstream (T04 and T08, respectively). Figure 11 is interesting because for three cases out of four (T04 North, T04 South, and T08 West) the turbulence intensity is observed to increase when the wind direction approaches the center of the wake, which is a reasonable result. For the T08 North case, the turbulence intensity is quite constant as a function of the direct distance from the wake center. This is most probably due to the effect of the terrain. It is interesting to notice that this kind of effect, which is somehow expected in complex terrain [47], indeed, occurs also in cases such as the one selected in this work, where the terrain is quite gentle. This result provides a qualitative indication of the fact that it is very likely that turbulence intensity and direction distance from the wake center are well-correlated quantities, but this is not assured and in general, those two quantities might convey slightly different information.

Figure 12 reports the difference between the power measurements of the downstream wind turbine in waked operation and the corresponding simulation in free stream conditions as a function of the angular distance with respect to the wake center. As described in general in Section 2 and specified in Section 3 for this test case, the free stream simulation for the target T04 or T08 wind turbines is obtained by generating the output of a data-driven model taking as input the power of the upstream wind turbine (see Table 4) when both wind turbines are upstream. In Figure 12, such a set of residuals is averaged per intervals of  $\theta_d$ , thus leading to the Angular Distance–Residual curve indicated in Table 1. Figure 12 quite fairly agree with Figure 11 because of the higher the turbulence intensity and the higher the wake losses. The most relevant loss occurs for T04 in the South sector at the center of the wake (up to 250 kW on average). It is interesting to notice that there is practically no loss when the absolute value of the direction distance with respect to the wake center is higher than  $20^\circ$ , for the T04 North, T04 South, and T08 West cases. Instead, for the T08 North case there is a relevant loss along all the wake sectors, which is likely related to the fact that the turbulence intensity does not decrease when the distance from

the wake center increases. The case of T04 South is further analyzed in Figure 13, where the residuals between model estimates and measurements are averaged per power intervals of the upstream wind turbine T03. From Figure 13, it arises that the wake losses are higher for powers of T03 higher than 2 MW. This can be seen as a different way of characterizing the behavior reported in Figure 9: in this case, using the relative performance with respect to the upstream wind turbine.

The wake losses reported in Figure 12 can then be averaged and reported to the measured AEP (Equation (5)), thus obtaining the estimates of Table 7. Coherently with the above results, the wake sectors non-negligibly affecting the AEP are T04 South and T08 North, i.e., those characterized by higher average turbulence intensity.

Finally, the analysis of the factors influencing the behavior under wake is pursued by determining the input variables which are required for modeling the power with the lowest possible error. As described in Section 2 and specified in Section 3, a Sequential Features Selection is employed starting from the dataset T04 South, which is selected because it is the most populated. The selected input variables are reported in Table 8. The level of turbulence intensity is accounted for by the presence of minimum, maximum, and standard deviations on the 10-minutes time interval. It is worth noticing that the distance from the wake center is selected as the input variable. This means that this variable provides additional information which is not merely already contained in the variability over the time interval of the rotational speed and the blade pitch.



**Figure 11.** The distribution of turbulence intensity as a function of the distance from the center of the waked sectors for the four test cases.

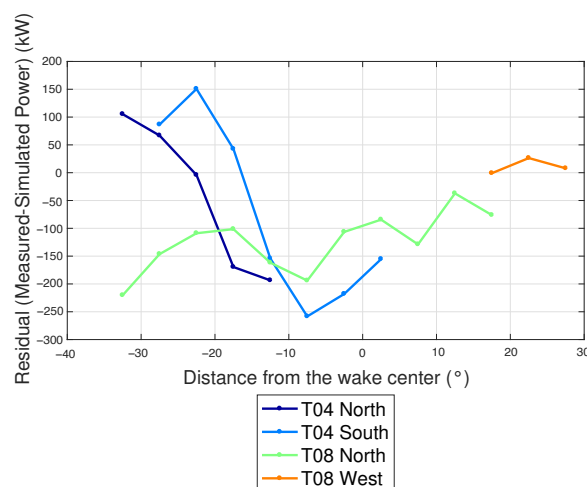


**Figure 12.** The distribution of the residuals between power measurements and simulations as a function of the distance from the center of the waked sectors for the four test cases.

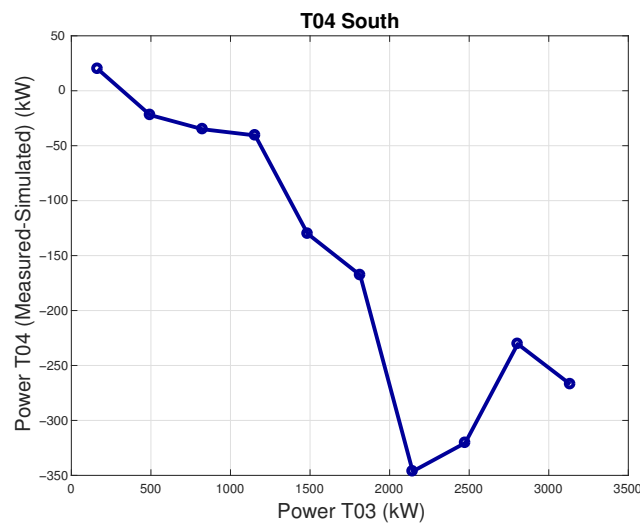


**Figure 13.** The residuals between model estimates and measurements for T04 South case, as a function of the power of the upstream wind turbine (T03).

**Table 7.** Wake losses in percentage of the AEP, as estimated from the data-driven model.

Case	Production Loss
T04 North	+0.11%
T04 South	−1.13%
T08 North	−0.59%
T08 West	+0.04%

**Table 8.** Selected input variables for modeling the power under wake operation.

Rotor Speed (Average, Minimum) (rpm)
Blade Pitch (Average, Minimum, Maximum, Std Dev) (°)
Direction Distance with respect to the wake center (°)

Finally, the so-obtained model is tested on a portion of the T04 South dataset and on the T04 North dataset. The accuracy metrics for such testing are reported in Table 9. It arises that the metrics for the T04 North dataset are only in the order of 10% higher than for the testing subset of the T04 South dataset. Considering that a part of the T04 South dataset is the training dataset and that the behavior of the T04 North wake sector is peculiar as regards the distribution of turbulence intensity (Figure 11), this result is remarkable in the sense that it tells that the set of input variables indicated in Table 8 captures features of the wake behavior that can be considered quite general.

**Table 9.** The accuracy metrics of the model for the power of wind turbine T04. The model is trained on two-thirds of the data from T04 South and tested on the remaining third and on the T04 North wake sector.

Metric	kW
MAE T04 South	56.3
MAE T04 North	61.1
RMSE T04 South	97.4
RMSE T04 North	107.1

## 5. Conclusions

This work has dealt with the characterization of wind turbine operation under wake through SCADA data analysis and has been organized as a real-world test case discussion. Actually, two wind turbines from an onshore wind farm have been selected and their behavior in the waked sectors has been analyzed and compared to the free stream operation. The general motivation of this work is that the identification of the key SCADA parameters describing the behavior of wind turbines in wake is an overlooked topic, which otherwise would be important for advanced wind farm control applications and for managing the power variability in case the wind farms are requested to contribute to grid ancillary services.

The characterization of wind turbine operation in wake has been pursued through the analysis of appropriate operation curves and through data-driven methods. The turbulence intensity is individuated as the key factor determining the observed behavior. Actually, the operation curve analysis highlights that a wind turbine in wake not only loses production because the wind intensity decreases while passing through the upstream rotor but also because, for a certain wind intensity, the higher turbulence induced by the wake stresses the wind turbine control. In particular, in the full aerodynamic load operation (i.e., when the wind turbine regulates the blade pitch and the rotational speed) the increased turbulence does not cause appreciable losses, while it does when the aerodynamic load is partial (i.e., the rotational speed is rated and the wind turbine regulates the load through the blade pitch). Indeed, a deviation of approximately  $1^\circ$  of blade pitch in the partial aerodynamic load region is observed for the wake sectors characterized by higher turbulence intensity.

The above interpretation has been confirmed by a data-driven model for the wake losses estimate, taking as input the power of the nearby wind turbine. The model is trained to learn the data-driven relation between a couple of nearby wind turbines when both are in free stream and is employed to simulate the output when the downstream wind turbine is in the wake of the upstream one. The difference between model estimates and measurements therefore allows for estimating the losses. It results that the wake losses are negligible for the two sectors with average turbulence intensity less than 10%, while the impact is meaningful for the two sectors (T04 South and T08 North) for which the average turbulence intensity is in the order of 13%.

The waked sectors have been subsequently characterized by analyzing how the turbulence intensity distributes as a function of the wind direction, specifically focusing on the proximity of wind intensity to the center of the wake. It was observed that, in general, the closer the direction to the center of the wake, the higher the turbulence intensity. However, it is important to consider the distance of the wind direction from the wake center and the turbulence intensity as separate factors when explaining the observed power variability. Terrain effects can make the relationship between these two quantities non-trivial also in the absence of evident complexity, as observed in this work in one of the analyzed waked sectors.

In general, therefore, the recommendation arising from this work is that a robust comprehension of how the power of wind turbine generators varies in the presence of wakes requires non-trivial data analysis methods. It should be taken into account that in an offshore environment there could be further factors to take into account, for example the influence of waves [48,49], but the approach proposed in this study can be easily generalized by including further features affecting the extracted power. The results of this study can be beneficial for further advancements in the general field of wake active control and for short or ultra-short-term wind power forecasts. Actually, for those applications, it is important to determine through real-world test cases what are the factors determining the behavior of wind farms in highly variable and highly uncertain operation conditions.

**Author Contributions:** Methodology, D.A. and F.D.C.; Software, D.A.; Validation, D.A. and F.D.C.; Formal analysis, A.V.; Writing—original draft, A.V. All authors have read and agreed to the published version of the manuscript.

**Funding:** This research received no external funding.

**Data Availability Statement:** Data may be obtained upon a reasonable request made to the Authors, subject to the requisite permission being obtained from ENGIE.

**Acknowledgments:** The authors thank the ENGIE Italia company for providing the data and for the technical support.

**Conflicts of Interest:** The authors declare no conflict of interest.

## Abbreviations

The following abbreviations are used in this manuscript:

AEP	Annual Energy Production
IEC	International Electrotechnical Commission
MAE	Mean Absolute Error
O& M	Operation & Maintenance
RMSE	Root Mean Square Error
SCADA	Supervisory Control And Data Acquisition
SFS	Sequential Features Selection
SVR	Support Vector Regression
TSO	Transmission System Operators
WTG	Wind Turbine Generator

## References

1. Barthelmie, R.J.; Hansen, K.; Frandsen, S.T.; Rathmann, O.; Schepers, J.; Schlez, W.; Phillips, J.; Rados, K.; Zervos, A.; Politis, E.; et al. Modelling and measuring flow and wind turbine wakes in large wind farms offshore. *Wind Energy Int. J. Prog. Appl. Wind Power Convers. Technol.* **2009**, *12*, 431–444. [[CrossRef](#)]
2. Gaumond, M.; Réthoré, P.E.; Bechmann, A.; Ott, S.; Larsen, G.C.; Peña, A.; Hansen, K.S. Benchmarking of wind turbine wake models in large offshore wind farms. In Proceedings of the Science of Making Torque from Wind Conference, Oldenburg, Germany, 9–11 October 2012.
3. Nilsson, K.; Ivanell, S.; Hansen, K.S.; Mikkelsen, R.; Sørensen, J.N.; Breton, S.P.; Henningson, D. Large-eddy simulations of the Lillgrund wind farm. *Wind Energy* **2015**, *18*, 449–467. [[CrossRef](#)]
4. Walker, K.; Adams, N.; Gribben, B.; Gellatly, B.; Nygaard, N.G.; Henderson, A.; Marchante Jiménez, M.; Schmidt, S.R.; Rodriguez Ruiz, J.; Paredes, D.; et al. An evaluation of the predictive accuracy of wake effects models for offshore wind farms. *Wind Energy* **2016**, *19*, 979–996. [[CrossRef](#)]
5. Sebastiani, A.; Castellani, F.; Crasto, G.; Segalini, A. Data analysis and simulation of the Lillgrund wind farm. *Wind Energy* **2021**, *24*, 634–648. [[CrossRef](#)]
6. Wu, Y.T.; Porté-Agel, F. Modeling turbine wakes and power losses within a wind farm using LES: An application to the Horns Rev offshore wind farm. *Renew. Energy* **2015**, *75*, 945–955. [[CrossRef](#)]
7. Hansen, K.S.; Barthelmie, R.J.; Jensen, L.E.; Sommer, A. The impact of turbulence intensity and atmospheric stability on power deficits due to wind turbine wakes at Horns Rev wind farm. *Wind Energy* **2012**, *15*, 183–196. [[CrossRef](#)]
8. Gaumond, M.; Réthoré, P.E.; Ott, S.; Peña, A.; Bechmann, A.; Hansen, K.S. Evaluation of the wind direction uncertainty and its impact on wake modeling at the Horns Rev offshore wind farm. *Wind Energy* **2014**, *17*, 1169–1178. [[CrossRef](#)]
9. Hasager, C.B.; Rasmussen, L.; Peña, A.; Jensen, L.E.; Réthoré, P.E. Wind farm wake: The Horns Rev photo case. *Energies* **2013**, *6*, 696–716. [[CrossRef](#)]
10. Cole, M.; Campos-Gaona, D.; Stock, A.; Nedd, M. A critical review of current and future options for wind farm participation in ancillary service provision. *Energies* **2023**, *16*, 1324. [[CrossRef](#)]
11. Zhong, C.; Wang, H.; Jiang, Z.; Tian, D. A unified optimization control of wind farms considering wake effect for grid frequency support. *Wind Eng.* **2023**, *47*, 0309524X231163823. [[CrossRef](#)]
12. Bhyri, A.K.; Senroy, N.; Saha, T.K. Enhancing the grid support from DFIG-Based wind farms during voltage events. *IEEE Trans. Power Syst.* **2023**, 1–12. [[CrossRef](#)]
13. Siniscalchi-Minna, S.; Bianchi, F.D.; De-Prada-Gil, M.; Ocampo-Martinez, C. A wind farm control strategy for power reserve maximization. *Renew. Energy* **2019**, *131*, 37–44. [[CrossRef](#)]
14. Singh, N.; De Kooning, J.D.; Vandeveld, L. Dynamic wake analysis of a wind turbine providing frequency support services. *IET Renew. Power Gener.* **2022**, *16*, 1853–1865. [[CrossRef](#)]
15. Guo, N.Z.; Shi, K.Z.; Li, B.; Qi, L.W.; Wu, H.H.; Zhang, Z.L.; Xu, J.Z. A physics-inspired neural network model for short-term wind power prediction considering wake effects. *Energy* **2022**, *261*, 125208. [[CrossRef](#)]

16. Wang, Y.; Shen, R.; Ma, Y.; Ma, M.; Zhou, Q.; Lu, Q.; Zhang, J. Research on Ultra-short term Forecasting Technology of Wind Power Output Based on Wake Model. *J. Phys. Conf. Ser.* **2022**, *2166*, 012041. [[CrossRef](#)]
17. Iungo, G.V.; Viola, F.; Camarri, S.; Porté-Agel, F.; Gallaire, F. Linear stability analysis of wind turbine wakes performed on wind tunnel measurements. *J. Fluid Mech.* **2013**, *737*, 499–526. [[CrossRef](#)]
18. Chamorro, L.P.; Porté-Agel, F. A wind-tunnel investigation of wind-turbine wakes: Boundary-layer turbulence effects. *Bound. Layer Meteorol.* **2009**, *132*, 129–149. [[CrossRef](#)]
19. Chamorro, L.P.; Porté-Agel, F. Effects of thermal stability and incoming boundary-layer flow characteristics on wind-turbine wakes: A wind-tunnel study. *Bound. Layer Meteorol.* **2010**, *136*, 515–533. [[CrossRef](#)]
20. Houck, D.R. Review of wake management techniques for wind turbines. *Wind Energy* **2022**, *25*, 195–220. [[CrossRef](#)]
21. Nash, R.; Nouri, R.; Vassel-Behagh, A. Wind turbine wake control strategies: A review and concept proposal. *Energy Convers. Manag.* **2021**, *245*, 114581. [[CrossRef](#)]
22. Makridis, A.; Chick, J. Validation of a CFD model of wind turbine wakes with terrain effects. *J. Wind Eng. Ind. Aerodyn.* **2013**, *123*, 12–29. [[CrossRef](#)]
23. Sandeise, B.; Van der Pijl, S.; Koren, B. Review of computational fluid dynamics for wind turbine wake aerodynamics. *Wind Energy* **2011**, *14*, 799–819. [[CrossRef](#)]
24. Castellani, F.; Vignaroli, A. An application of the actuator disc model for wind turbine wakes calculations. *Appl. Energy* **2013**, *101*, 432–440. [[CrossRef](#)]
25. Dar, A.S.; Porté-Agel, F. An analytical model for wind turbine wakes under pressure gradient. *Energies* **2022**, *15*, 5345. [[CrossRef](#)]
26. Vahidi, D.; Porté-Agel, F. A physics-based model for wind turbine wake expansion in the atmospheric boundary layer. *J. Fluid Mech.* **2022**, *943*, A49. [[CrossRef](#)]
27. Pandit, R.; Astolfi, D.; Hong, J.; Infield, D.; Santos, M. SCADA data for wind turbine data-driven condition/performance monitoring: A review on state-of-art, challenges and future trends. *Wind Eng.* **2023**, *47*, 422–441. [[CrossRef](#)]
28. Chesterman, X.; Verstraeten, T.; Daems, P.J.; Nowé, A.; Helsen, J. Overview of normal behavior modeling approaches for SCADA-based wind turbine condition monitoring demonstrated on data from operational wind farms. *Wind Energy Sci.* **2023**, *8*, 893–924. [[CrossRef](#)]
29. Mittelmeier, N.; Allin, J.; Blodau, T.; Trabucchi, D.; Steinfeld, G.; Rott, A.; Kühn, M. An analysis of offshore wind farm SCADA measurements to identify key parameters influencing the magnitude of wake effects. *Wind Energy Sci.* **2017**, *2*, 477–490. [[CrossRef](#)]
30. Gonzalez, E.; Valldecabres, L.; Seyr, H.; Melero, J. On the effects of environmental conditions on wind turbine performance: An offshore case study. *J. Phys. Conf. Ser.* **2019**, *1356*, 012043. [[CrossRef](#)]
31. Hammer, F.; Helbig, N.; Losinger, T.; Barber, S. Graph machine learning for predicting wake interaction losses based on SCADA data. *J. Phys. Conf. Ser.* **2023**, *2505*, 012047. [[CrossRef](#)]
32. Ciulla, G.; D’Amico, A.; Di Dio, V.; Brano, V.L. Modelling and analysis of real-world wind turbine power curves: Assessing deviations from nominal curve by neural networks. *Renew. Energy* **2019**, *140*, 477–492. [[CrossRef](#)]
33. Astolfi, D. Perspectives on SCADA data analysis methods for multivariate wind turbine power curve modeling. *Machines* **2021**, *9*, 100. [[CrossRef](#)]
34. Carullo, A.; Ciocia, A.; Malgaroli, G.; Spertino, F. An Innovative Correction Method of Wind Speed for Efficiency Evaluation of Wind Turbines. *Acta Imeko* **2021**, *10*, 46–53. [[CrossRef](#)]
35. Honrubia, A.; Viguera-Rodríguez, A.; Gómez-Lázaro, E. The influence of turbulence and vertical wind profile in wind turbine power curve. In *Progress in Turbulence and Wind Energy IV*; Springer: Berlin/Heidelberg, Germany, 2012; pp. 251–254.
36. Hedeveang, E. Wind turbine power curves incorporating turbulence intensity. *Wind Energy* **2014**, *17*, 173–195. [[CrossRef](#)]
37. Astolfi, D. Wind Turbine Operation Curves Modelling Techniques. *Electronics* **2021**, *10*, 269. [[CrossRef](#)]
38. Zhang, Y.; Li, Z.; Liu, X.; Sotiropoulos, F.; Yang, X. Turbulence in waked wind turbine wakes: Similarity and empirical formulae. *Renew. Energy* **2023**, *209*, 27–41. [[CrossRef](#)]
39. De Cillis, G.; Cherubini, S.; Semeraro, O.; Leonardi, S.; De Palma, P. The influence of incoming turbulence on the dynamic modes of an NREL-5MW wind turbine wake. *Renew. Energy* **2022**, *183*, 601–616. [[CrossRef](#)]
40. Gasch, R.; Tvele, J. *Wind Power Plants: Fundamentals, Design, Construction and Operation*; Springer Science & Business Media: Berlin/Heidelberg, Germany, 2011.
41. IEC. *Power Performance Measurements of Electricity Producing Wind Turbines*; Technical Report 61400–12; International Electrotechnical Commission: Geneva, Switzerland, 2005.
42. De Caro, F.; Vaccaro, A.; Villacci, D. Adaptive wind generation modeling by fuzzy clustering of experimental data. *Electronics* **2018**, *7*, 47. [[CrossRef](#)]
43. Pandit, R.; Kolios, A. SCADA Data-Based Support Vector Machine Wind Turbine Power Curve Uncertainty Estimation and Its Comparative Studies. *Appl. Sci.* **2020**, *10*, 8685. [[CrossRef](#)]
44. Dhiman, H.S.; Deb, D.; Carroll, J.; Muresan, V.; Unguresan, M.L. Wind turbine gearbox condition monitoring based on class of support vector regression models and residual analysis. *Sensors* **2020**, *20*, 6742. [[CrossRef](#)]
45. Vidal, Y.; Pozo, F.; Tutivén, C. Wind turbine multi-fault detection and classification based on SCADA data. *Energies* **2018**, *11*, 3018. [[CrossRef](#)]
46. Astolfi, D.; De Caro, F.; Vaccaro, A. Condition Monitoring of Wind Turbine Systems by Explainable Artificial Intelligence Techniques. *Sensors* **2023**, *23*, 5376. [[CrossRef](#)] [[PubMed](#)]

47. Elgendi, M.; AlMallahi, M.; Abdelkhalig, A.; Selim, M.Y. A review of wind turbines in complex terrain. *Int. J. Thermofluids* **2023**, *17*, 100289. [[CrossRef](#)]
48. Xiao, S.; Yang, D. Large-eddy simulation-based study of effect of swell-induced pitch motion on wake-flow statistics and power extraction of offshore wind turbines. *Energies* **2019**, *12*, 1246. [[CrossRef](#)]
49. Sacie, M.; Santos, M.; López, R.; Pandit, R. Use of state-of-art machine learning technologies for forecasting offshore wind speed, wave and misalignment to improve wind turbine performance. *J. Mar. Sci. Eng.* **2022**, *10*, 938. [[CrossRef](#)]

**Disclaimer/Publisher's Note:** The statements, opinions and data contained in all publications are solely those of the individual author(s) and contributor(s) and not of MDPI and/or the editor(s). MDPI and/or the editor(s) disclaim responsibility for any injury to people or property resulting from any ideas, methods, instructions or products referred to in the content.